scientific reports

Check for updates

OPEN

Profiling of RNA N6-Methyladenosine methylation reveals the critical role of m6A in betaine alleviating hepatic steatosis

Yuna Wu[1,3], Jingsu Yu[1,3], Haisen Song[1], Dehao Lu[1], Zhilin Li[1], Xiangling Li[1], Zhaoxuan Ding[1], Lei Zhou[1], Jie Ma[1], Ying Zhang[2] & Yixing Li[1]✉

Metabolic dysfunction-associated steatotic liver disease (MASLD) is a major predisposing factor of metabolic dysfunction-associated steatohepatitis, hepatic fibrosis and hepatocellular carcinoma. Abnormal RNA m6A modification leads to the disturbance of lipid metabolism, insulin resistance, and chronic inflammation, all of which are critical for the onset and progression of MASLD. It has been shown that betaine supplementation has an ameliorative effect on symptoms associated with MASLD. The purpose of this study is to explore the role of RNA m6A modification in the alleviation of MASLD by betaine, and to find out the possible targets of betaine. Methylated RNA immunoprecipitation sequencing (MeRIP-seq) and RNA sequencing (RNA-seq) were respectively employed to contrast m6A methylation profiles of livers from high-fat diet mice with betaine supplementation vs. those without betaine supplementation (HB vs. HFD). Functional enrichment analysis showed that up-methylated genes are mainly related to mTOR signaling pathway, Rap1 signaling pathway and MAPK signaling pathway. In addition, differentially expressed mRNAs were enriched in pathways such as promoting lipid catabolism and reducing lipid accumulation. By combining analyses of MeRIP-seq and RNA-seq, we identified 27 genes exhibiting significant differences in m6A abundance and mRNA levels. Notably, a new candidate gene, *Trub2*, was screened out and identified. Inhibition of *Trub2* increased intracellular TG levels in AML12 cells, and this promotion was reduced by betaine, suggesting that betaine reduces intracellular TG levels by increasing *Trub2* expression. Our findings in this study provide a new target and a new approach for the treatment of MASLD.

Keywords Betaine, MASLD, N6-methyladenosine (m6A), MeRIP-seq, Trub2

MASLD is a chronic liver disease characterized by lipid accumulation and hepatocyte steatosis[1]. It is the most important factor in a range of serious metabolic diseases, including nonalcoholic steatohepatitis (NASH), liver fibrosis, cirrhosis, and even hepatocellular carcinoma (HCC)[2,3]. The incidence of MASLD has increased year by year, and it has become the largest chronic liver disease in the world, affecting about 25%~30% of the global population[4]. Similarly, the reported prevalence of MASLD has reached 29.2% in China, which has emerged as a major public health issue[5]. However, no specific drug has been found to be effective in the treatment of MASLD. Therefore, there is an urgent need to further explore the mechanism of action of MASLD and develop new therapeutic targets.

N6-methyladenosine (m6A) methylation, the most prevalent internal modification in eukaryotic mRNA, has been reported to be functional in many physiological events[6,7]. Proteins such as methyltransferases (writer), demethylases (eraser), and reader proteins (readers) work together to regulate the dynamic reversible modification of m6A[8]. m6A methyltransferase is responsible for catalyzing the formation of the m6A modification, by some methyltransferase-like 3 (METTL3)/ methyltransferase-like 14 (METTL14) heterologous dimers and various

[1]Guangxi Key Laboratory of Animal Breeding, Disease Control and Prevention, College of Animal Science and Technology, Guangxi University, Nanning 530004, China. [2]School of Life Sciences, Biodiscovery Institute, University of Nottingham, University Park, Nottingham NG7 2RD, UK. [3]Yuna Wu and Jingsu Yu contributed equally to this work. ✉email: liyixing39@gxu.edu.cn

other methyltransferase complexes[9].Demethylase catalyzes the removal of methyl groups on m6A, which are composed of the fat mass and obesity associated (FTO) and alkylation repair homolog protein 5 (ALKBH5)[10]. In patients with non-alcoholic fatty liver disease and in mouse models of MASLD, overexpression of FTO promotes hepatic steatosis and lipid accumulation[11].m6A methylated reading proteins, including YT521-B homology (YTH) domain-containing proteins (YTHDF1-3, YTHDC1-2) and Insulin-like growth factor 2 mRNA-binding proteins 1/2/3 (IGF2BP1/2/3), play a crucial role in the alternative splicing, stability, degradation and translation of mRNA by recognizing m6A modifications on RNA[10]. Hu et al. found that IGF2BP3 enhanced the mRNA stability of protein kinase, membrane-associated tyrosine/threonine 1 (PKMYT1) through its m6A modification site, thus promoting the development of gastric cancer[12]. Mu et al. found that IGF2BP1 mediates oxidative stress-induced granule-cell dysfunction by regulating murine double minute 2 (MDM2) mRNA stability in an m6A-dependent manner[13]. Given the critical role RNA m6A methylation plays in dysregulated lipid metabolism, it is consequently considered a highly promising and substantial therapeutic target.

Betaine (N, N, N-trimethylglycine), a trimethyl derivative of glycine, was first found in common plants in the 19th century[14]. As a natural methyl donor, betaine serves as an indispensable component in the metabolic regulation of organisms, playing a critical role in both glycemic-lipid metabolism and hepatic function regulation[15]. A significant amount of data from animal models of liver disease indicates that administration of betaine can halt and even reverse progression of the disruption of liver function[16]. In recent years, many pathways have been shown to be closely related to the improvement of MASLD by betaine, including inhibiting inflammatory responses, reducing oxidative stress in the liver, promoting fatty acid oxidation, improving insulin resistance, and regulating epigenetic modifications[17]. At the same time, clinical trials have shown that patients with NASH who receive purified betaine for up to one year can reduce their liver steatosis index[18]. However, the exact mechanism by which betaine participates in post-transcriptional regulation through m6A methylation and exerts its beneficial effects remains to be elucidated.

This research delineates a comprehensive map of the role played by betaine-induced m6A RNA methylation in attenuating hepatic steatosis, and it identifies *Trub2* as a target gene subject to m6A modification. This discovery furnishes a novel therapeutic target for investigating the mechanism by which betaine modulates lipid metabolism in the liver. This pioneering study offers a comprehensive depiction of the transcriptome-wide m6A modification pattern exerted by betaine in mitigating fatty liver degeneration, forging a connection between m6A and mRNA. It thereby provides a foundational basis for exploring how betaine alleviates MASLD through modulation of m6A modifications.

Method

Experimental animals and sample collection

All animal experiments were approved by the Committee on the Ethics of Animal Experiments of Guangxi University (No. GXU2019-063). A total of 12 eight-week-old male C57BL/6 mice with comparable body weights were randomly assigned to two groups: the high fat diet (HFD) group, and the high fat diet with betaine (HB) group, each consisting of six mice. Mice were housed in a facility with 12-h light/12-h dark cycle at 23 ± 3 °C and 30–70% humidity. In this study, HFD mice were given a high-fat diet (45% kcal fat; Jiangsu Medicience Ltd., Jiangsu, China), while the HB group was on the same high-fat diet but with added 2% w/v betaine in drinking water. Mice in the HFD group developed MASLD, while those in the HB group showed significant improvement in MASLD[19]. These findings have been thoroughly validated. After 17 weeks of dietary intervention, the mice inhaled isoflurane in a closed room, quickly reached an effective concentration (5%) and were euthanized[20]. All research involving animal experimentation was conducted in accordance with the National Institutes of Health guidelines on animal care and use. All methods are reported in accordance with ARRIVE guidelines.

RNA extraction

Total RNA was extracted from liver tissue using TRIzol reagent and the extracted lysed RNA was transferred to 1.5 ml RNase-free EP tubes. 100 *μl* of chloroform was added, and the mixture was shaken vigorously in a shaker for 15 s, left at room temperature, centrifuged. The upper water phase was taken and placed in a new EP tube, each tube was added with equal volume isopropyl alcohol, shaken well, standing, centrifuged. Then, the RNA was washed with anhydrous ethanol diluted with DEPC water, centrifuged, and the supernatant was discarded. The RNA concentration and purity were detected by using an enzyme-labeling instrument. The remaining RNA was stored at −80°C for subsequent library construction and high-throughput sequencing[19].

RNA dot blot

Cut the nitrocellulose (NC) membranes (Biosharp) and soak them in 20X Saline-Sodium Citrate Buffer (20X SSC, Biosharp) for 1 h. Dilute the RNA and mix it 1:1 with the denaturing solution (20X SSC: 37% deionized formaldehyde = 3:2, v/v), then heat it at 95 °C for 5 min to denature. Spot RNA samples (100 ng, 200 ng, and 400 ng) onto the NC membranes. After UV cross-linking, block the membrane with 1% Bovine Serum Albumin (BSA, Solarbio) for 1 h at room temperature. Incubate the membrane with anti-m6A antibody (1:2000, Beyotime) overnight at 4 °C, followed by incubation with the secondary antibody for 1 h. Detect the signal using a chemiluminescence technique after washing with PBST. As a loading control, stain the membranes in 0.3 mol/L sodium acetate (pH 5.2) containing 0.02% methylene blue.

Library construction, MeRIP-seq and RNA-seq

The quality of total mRNA and m6A-enriched RNA was detected by 2.5% agarose gel electrophoresis. m6A antibody-immunoprecipitated RNA underwent quality control using Qubit®3.0 (Thermo Fisher Scientific) and Agilent 2200 TapeStation. The qualified RNA was then used for library construction according to the NEBNext® Ultra™ RNA Library Prep Kit protocol for Illumina platforms (NEB). Post-library preparation, products were

evaluated with Agilent 2200 TapeStation and Qubit®3.0 before sequencing on an Illumina HiSeq X Ten platform with paired-end standard sequencing. High-throughput sequencing was performed on qualified mRNA and m6A-modified RNA. According to the protocol of VAHTS mRNA-seq and library preparation kit, the original sequencing reads were generated on the HiSeq X Ten sequencer.

Bioinformatics analysis

For mRNA and m6A sequencing datasets, high-quality reads were mapped to RefSeq mRNA reference sequences (mm10) using the FANSe2 algorithm. The reads mapped to variable splicing variants of a gene were merged. The abundance of mRNA and m6A in each sample was normalized per kilobase per million reads (RPKM)[21]. The differentially expressed genes (DEGs) were selected with the standard of absolute |Log2 fold change| ≥ 1 and $P < 0.05$ via R package edgeR. Kyoto Encyclopedia of Genes and Genomes (KEGG[22,23]) enrichment, Gene Ontology (GO) analysis and Reactome Gene Sets analysis were performed using the Metascape online tools (http://metascape.org/gp/index.html#/main/step1).

Construction of mouse *Trub2* overexpression plasmid

The result of enzyme digestion showed a band length of about 996 bp, which was consistent with the expected length, indicating that the CDS region fragment of mouse *Trub2* gene (NM_145520.5) was successfully constructed. The *Trub2* expression plasmid was constructed, and the primer sequences used for amplification were respectively AAGCTGGCTAGTTAAGCTTGCCACCATGGGTTTC (positive) and TCCGAGCTCGGT ACAAGCTTTTTACTGCC (reverse). The plasmid was transfected transiently with Liposome 3000 reagent[24].

Cell culture and transfection

AML12 cells were maintained in Dulbecco's modified Eagle's Ham's F-12 supplemented with 10% fetal bovine serum, ITS Liquid Media Supplement, and dexamethasone (40 ng ml^{-1}) under an atmosphere of 5% CO_2 at 37℃[25]and in an environment supplemented with 10% fetal bovine serum and 5% carbon dioxide. When the fusion rate reached 80%, the cells were seeded into the 24-well plate[26]. Cells were cultivated until they reached a density of approximately 80% confluence, at which point they were subjected to a 24-hour exposure to a mixture of oleic and palmitic acids (OA/PA) with the aim of inducing fat deposition. DMEM medium enriched with 200 μM oleic acid (OA) and 100 μM palmitic acid (PA) was employed to replicate the high-fat diet milieu in a cellular context. 2 mM betaine (Beijing Solarbio Science & Technology Co., Ltd. Beijing, China) was used to treat AML12 cells supplemented with OA/PA medium.

Upon reaching 60% confluence, cells were switched to serum-free DMEM (Gibco) and transfected with plasmids or siRNA using Hieff TransTM Liposomal Transfection Regent. The pcDNA3.1 or *Trub2* plasmid were transfected into AML12 cells. AML12 cells were transfected with siTrub2, or the negative control siRNA (siNC). The previously confirmed siRNA targeting sequences used in this study. siRNAs sequences are found in Table S1.

Real time quantitative PCR

According to the manufacturer's protocol, reverse transcription was performed to convert total RNA into cDNA, followed by quantitative PCR (qPCR) analysis on the Roche LightCycler® 480 Real-Time PCR system. So, all primers were synthesized by Qingke Biotech Co., Ltd (Beijing, China). β-actin gene was used as an internal reference gene. The $2^{-\Delta\Delta Ct}$ method was used to analyze the relative mRNA expression levels of genes. For this experiment, four biological repeats and technical repetitions were performed. Table S2 contains the necessary primer sequences.

Western blotting

Cultured AML12 cells were lysed with RIPA lysate. After centrifugation, the protein concentration was measured and diluted to 1 $\mu g/\mu l$, and 2X Laemmli loading buffer was added to load the buffer. The sample was boiled for 10 min, quickly frozen and stored at −20℃. The 20 μg protein was isolated with 10% SDS-PAGE gel and transferred to a PVDF membrane (Bio-Rad). The membranes were then cleaned with TBS-Tween and sealed with a sealer made of skim milk powder (5% skim milk powder) for 1 h. After blocking , the membranes were washed with TBST. The membranes were divided into two groups and incubated with the antibody against *alpha-tubulin* (Proteintech, China, 1:10,000 dilution), the antibody against *β-actin* (Proteintech, China, 1:10,000 dilution) and the antibody against *Trub2* (Proteintech, China, 1:2000 dilution).

Statistical analysis

The experimental results are expressed as mean ± SD[27].SPSS 20.0 software (SPSS Inc., Chicago, IL, USA) was used to conduct t-tests to analyze the significance of intergroup differences, and one-way analysis of variance (ANOVA) was performed on two or more groups. Significance is represented by an asterisk: $^{*}P < 0.05$, $^{**}P < 0.01$ and $^{****}P < 0.0001$.

Results

Differential m6A methylation analysis between HFD and HB groups

In order to investigate the disparity in m6A modification between the HFD and HB groups, we initially identified genes exhibiting significantly distinct m6A peaks between the two cohorts. We found 2,035 common genes in the HB group compared to the HFD group, with significant differences in their m6A peaks. A total of 934 genes exhibited up-regulated m6A methylation levels, while 1,101 genes showed down-regulated m6A methylation (Fig. 1A).

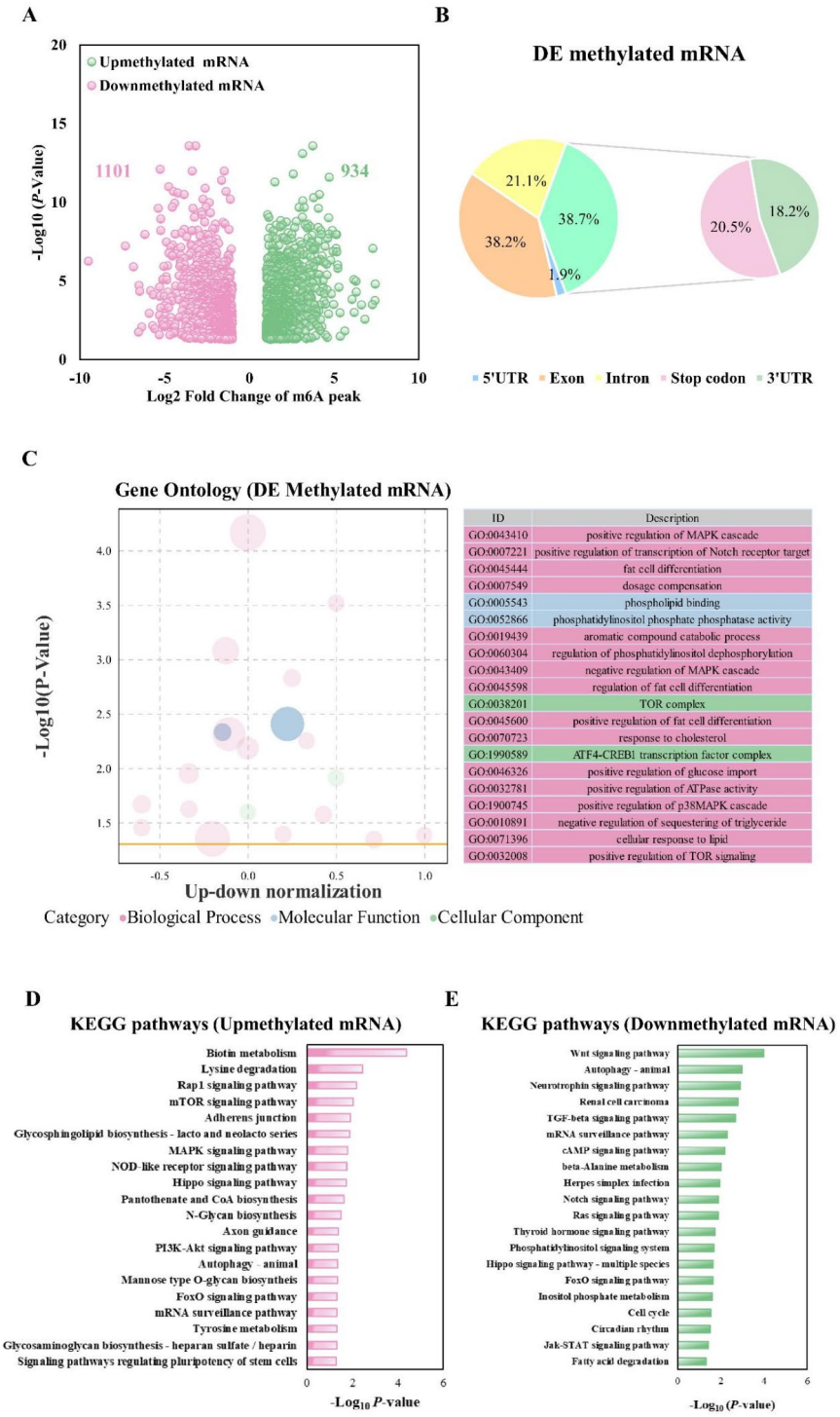

Fig. 1. The landscape of m6A methylation in the HFD and HB groups. **(A)** Volcano plot of differentially expressed m6A methylation mRNAs. **(B)** The pie chart shows the percentage of m6A peaks in the five non-overlapping segments of the mRNA transcript. **(C)** GO enrichment analysis showed the top 20 functional analyses of enriched differentially methylated mRNAs ($P < 0.05$). **(D)** KEGG pathway analysis showed the top 20 pathways of Upmethylated mRNAs ($P < 0.05$). **(E)** KEGG pathway analysis revealed the top 20 pathways of Downmethylated mRNAs ($P < 0.05$). HFD, High fat diet; HB, High fat diet with betaine; GO, Gene Ontology; KEGG, Encyclopedia of Genes and Genomes.

Distribution of m6A peaks on gene functional elements

To identify the primary m6A localization within transcripts, we partitioned the m6A peak into five distinct and non-overlapping segments: 5'-untranslated regions (5' UTR), exon, intron, stop codon, and 3'-untranslated regions (3' UTR). Our results indicate that the differentially methylated m6A peak is predominantly concentrated in the vicinity of the stop codon and 3' UTR (38.7%), where the stop codon accounts for 20.5% and the 3' UTR accounts for 18.2%, sometimes also near the exon (38.2%) (Fig. 1B), which is consistent with previous experimental results[28].

Analysis of differential methylation enrichment pathway between HFD and HB groups

To deepen our comprehension of the involvement of m6A modifications in the pathogenesis of MASLD, we carried out GO and KEGG[22,23] pathway enrichment analyses on genes exhibiting significant differential m6A methylation patterns. GO analysis indicated that differentially m6A methylated mRNAs were significantly enriched in biological processes such as positive regulation of mitogen-activated protein kinase (MAPK) cascade, positive regulation of Notch receptor target gene transcription and dosage compensation. In terms of molecular function, it is enriched in phospholipid binding and phosphatidylinositol phosphate phosphatase activity. In terms of cell components, target of rapamycin (TOR) complex and Activating transcription factor 4 - the cAMP response element binding protein 1 (ATF4-CREB1) transcription factor complex are enriched. In particular, a large number of differential m6A methylation genes are involved in the positive regulation of the mitogen-activated protein kinase (MAPK) cascade, phospholipid binding, and aromatic compound catabolic process (Fig. 1C). Some of the pathways mentioned above are associated with MASLD progression, such as phospholipid binding[29], and phosphatidylinositol phosphate phosphatase activity[30].

KEGG pathway analysis disclosed that mRNAs subject to upregulated m6A methylation predominantly implicated the mechanistic target of rapamycin (mTOR) signaling cascade, the Ras-related protein 1 (Rap1) signaling pathway, and MAPK signaling pathway (Fig. 1D). mRNAs experiencing downregulated m6A methylation were predominantly associated with the wingless/integrated (Wnt) signaling pathway, neurotrophic factor signaling pathways, and transforming growth factor-beta (TGF-β) signaling cascades (Fig. 1E). mTOR signaling pathway is involved in inducing autophagy to reduce hepatic steatosis and promote fatty acid oxidation[31]. Studies have shown that CD147 reprograms fatty acid metabolism in hepatocellular carcinoma cells through Akt/mTOR/SREBP1c and P38/PPARα pathways[32]. Deletion of Telomere-Rap1 aggravated cardiac aging by imparing fatty acid oxidation via PPARα signaling[33]. In addition, Qin et al. found that isoquercetin improved hepatic lipid accumulation in HFD-induced nonalcoholic fatty liver rat models by activating AMP-activated protein kinase (AMPK) pathway and inhibiting TGF-β signaling[34], which is very consistent with our findings. Taken together, these data suggest that the underlying mechanism of m6A methylation in betaine in alleviating the progression of MASLD is closely related to the disorder of glucose and lipid metabolism and the activation of liver inflammatory response, but further evidence is needed to support this.

Differential transcriptome and functional analysis between HFD and HB groups

To investigate the relationship between gene expression and phenotype, transcriptome differential analysis was conducted for the HFD and HB groups. A total of 348 DEGs were analyzed, with 173 up-regulated genes and 175 down-regulated genes, respectively (Fig. 2A). In the GO functional enrichment analysis, DEGs were significantly enriched in biological processes such as lipid biosynthesis, small molecule biosynthesis, lipid metabolism, and small molecule metabolism. Among them, the processes of cholesterol biosynthetic process, secondary alcohol biosynthetic process and sterol biosynthetic process are highly significant and reliable (Fig. 2B). In the KEGG[22,23] enrichment analysis, DEGs were found to be mainly involved in pathways related to metabolism, human diseases, environmental information processing, and cellular processes. These included 36 genes associated with signal transduction mechanisms, 31 genes implicated in lipid metabolism, 22 genes relevant to endocrine and metabolic disorders, and 13 genes involved in carbohydrate metabolism pathways (Fig. 2C). Reactome Gene Sets showed that in mRNAs with upregulated expression, DEGs were mainly enriched in reactions such as cholesterol biosynthesis[35], metabolism of lipids, metabolism of steroids[36]and fatty acyl-coenzyme A (acyl-CoA) biosynthesis[37]. DEGs of downregulated mRNAs were mainly enriched in responses such as Generic Transcriptional pathway, Estrogen-dependent gene expression[38], and ESR-mediated signaling[39] (Fig. 2D, E). In summary, compared to the HFD group, the HB group displays an upregulated expression level for a substantial number of reactions implicated in liver lipid metabolism, particularly those promoting accelerated lipid catabolism and mitigating hepatic lipid accumulation.

Combined analysis of enrichment pathways of differentially methylated genes and differentially expressed genes

To elucidate the relationship between differentially methylated genes and differentially expressed genes, we initially discerned the expression upregulation pathways in which they both participate. In the context of GO Biological Processes, we ascertained that 670 distinct processes were engaged by differentially methylated mRNAs, while 244 processes were implicated in differentially expressed mRNAs. In particular, there were 31 biological processes (7.28%) between the two groups, among which the mRNA methylation of negative regulation of phosphorus metabolic process was significantly different (Fig. 3A, B). These results suggest that the methylation status of mRNA associated with negative regulation of phosphorus metabolism was significantly altered after betaine administration. The KEGG[22,23] pathway analysis unveiled that 23 pathways were linked to differentially expressed methylated mRNAs, and 17 pathways were associated with differentially expressed mRNAs. Among these, 1 pathway (5.26%) was common to both sets, the alcoholic liver disease pathway (Fig. 3C, F). Per the Wiki pathway resource, 17 pathways were connected to differentially expressed methylated mRNAs, and 14 pathways were relevant to differentially expressed mRNAs, with 2 pathways (14.81%) being mutual to

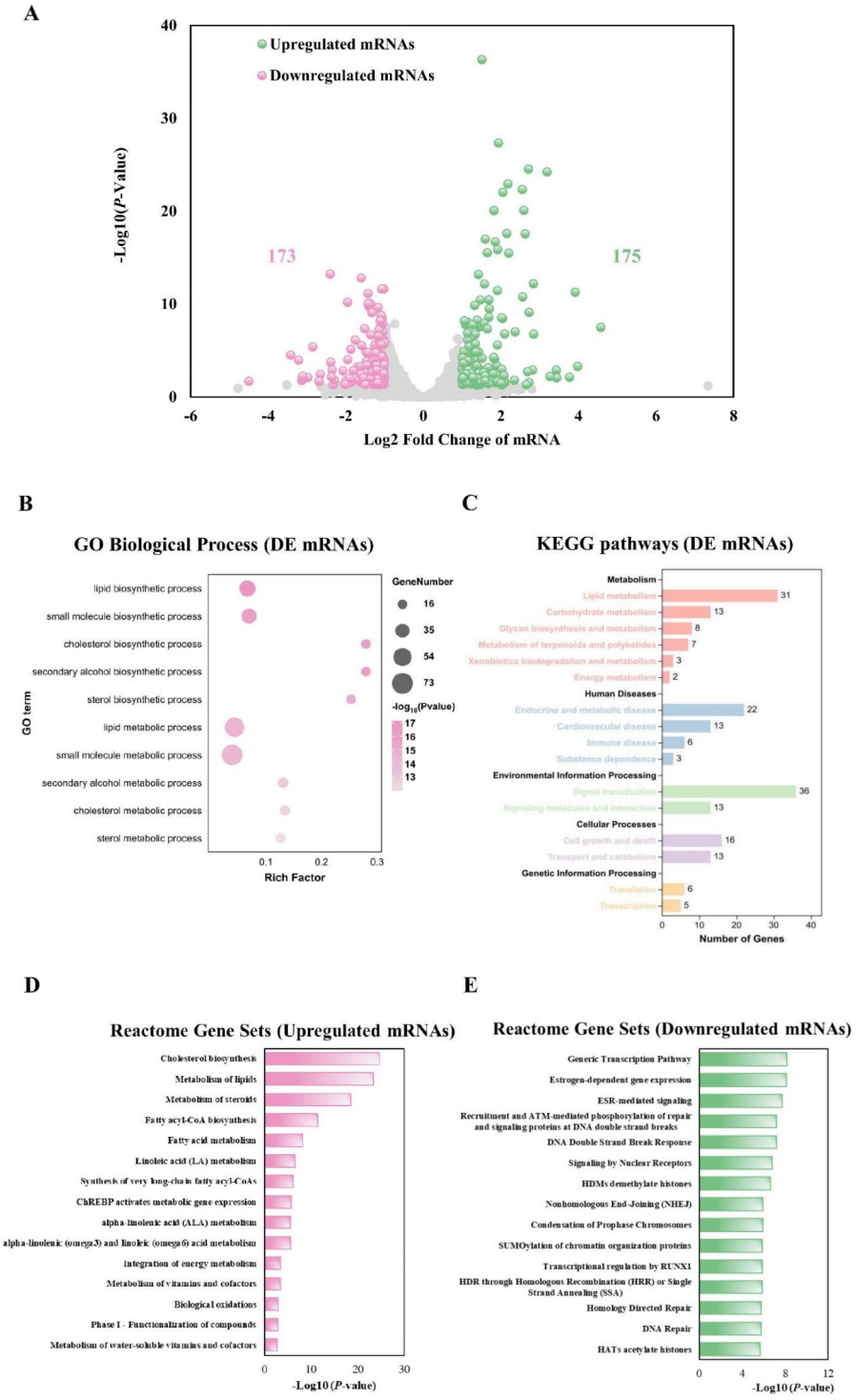

Fig. 2. Transcriptional differences between HFD and HB groups. **(A)** Volcano map of differentially expressed mRNAs. **(B)** GO enrichment analysis showed the top 10 functional analyses of enriched differential mRNAs ($P < 0.05$). **(C)** The number of differential genes enriched by different types of pathways on KEGG ($P < 0.05$). **(D)** Reactome Gene Sets showed the top 15 pathways of upregulated mRNAs ($P < 0.05$). **(E)** Reactome Gene Sets showed the top 15 pathways of downregulated mRNAs ($P < 0.05$).

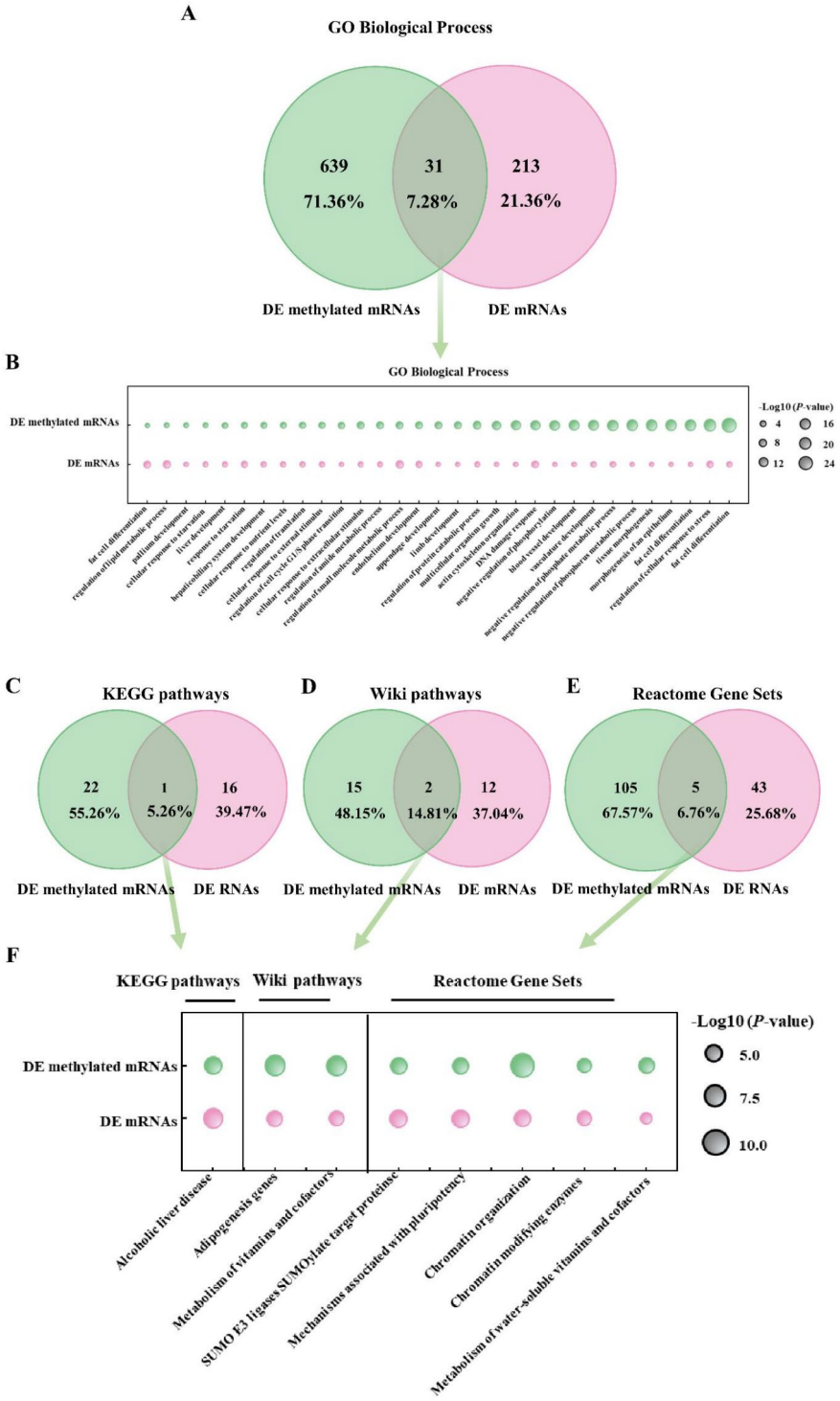

Fig. 3. Venn diagram of overlapped genes of DE methylated mRNAs and DE mRNAs and their pathways. **(A)** The Venn diagram showed the overlap among GO biological processes of DE methylated mRNAs and DE mRNAs. **(B)** Bubble plots showed pathways for overlapping genes in GO biological processes. **(C)** The Venn diagram showed the overlap of pathways in KEGG among DE methylated mRNAs and DE mRNAs. **(D)** The Venn diagram showed the overlap of pathways in Wiki among DE methylated mRNAs and DE mRNAs. **(E)** The Venn diagram showed the overlap of pathways in Reactome Gene Sets among DE methylated mRNAs and DE mRNAs. **(F)** Bubble plots showed pathways in which genes overlap in KEGG, Wiki, Reactome Gene Sets. DE, differentially expressed.

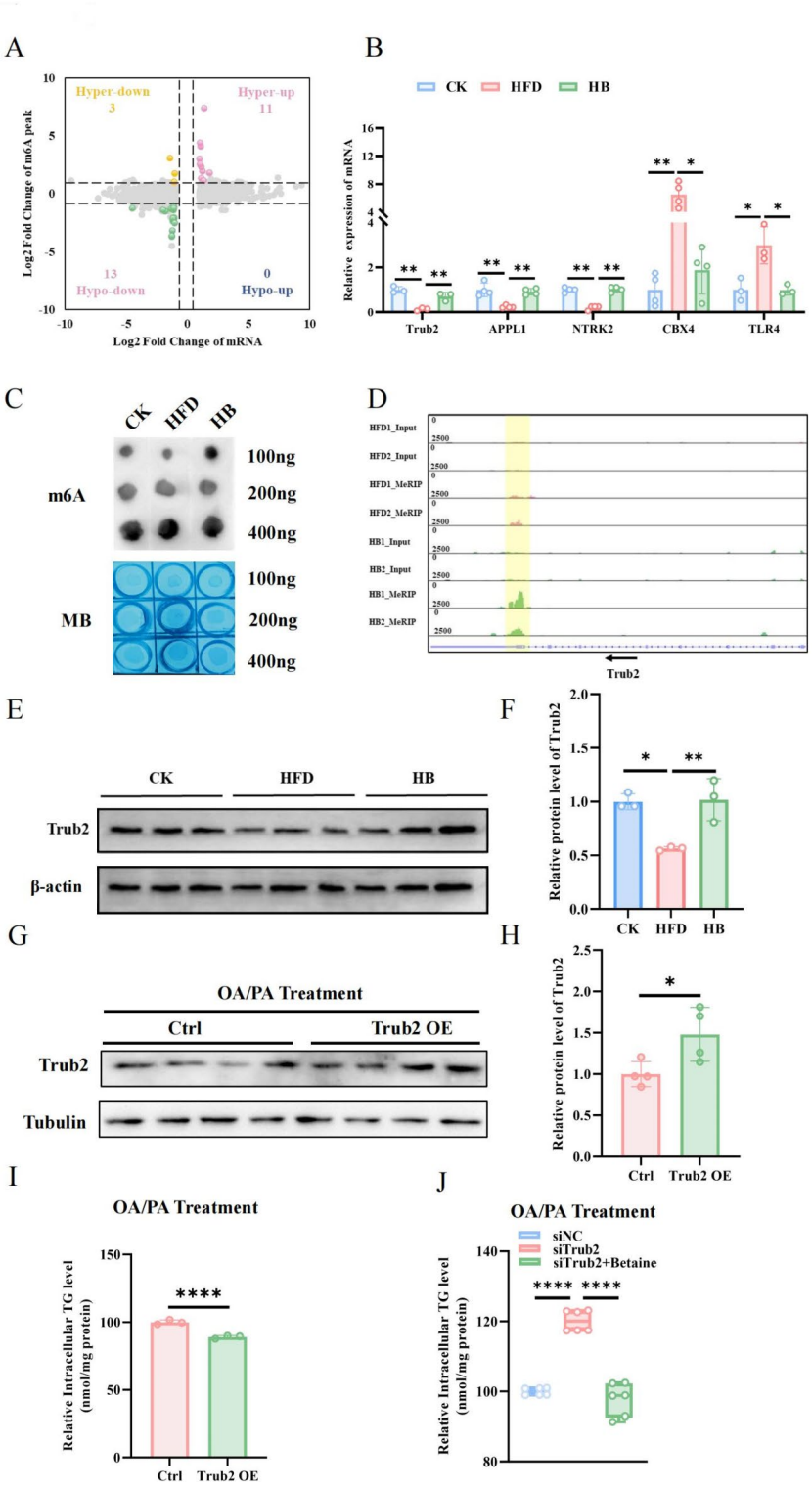

both, namely, lipogenesis gene networks and metabolic pathways of vitamins and cofactors (Fig. 3D, F). Lastly, Reactome Gene Sets demonstrated that 110 pathways were involved in differentially expressed methylated mRNAs, and 48 pathways pertained to differentially expressed mRNAs. Of these, 5 pathways (6.76%) were common to both categories, all pertaining to chromatin organization (Fig. 3E, F).

In summary, relative to the HFD group, the HB group exhibits elevated m6A levels and mRNA expression in lipid metabolism and negative regulation of phosphorus metabolism[40]. This suggests that betaine may regulate the stability of mRNA by mobilizing these pathways, affect the metabolic process, and thus inhibit lipid accumulation, thereby inhibiting the formation of obesity and reducing fatty liver.

◀**Fig. 4**. **(A)** The four-quadrant plots showed significant changes in mRNA expression and m6A methylation in gene distribution. **(B)** The mRNA level of *Appl1*, *Ntrk2*, *Trub2*, *Cbx4* and *Tlr4* ($n = 3$ or 4). **(C)** Dot blot detecting the global m6A modification of mRNAs. Methylene blue (MB) staining was used as a loading control. Gel images were cropped, and the original gels were presented in Supplementary **Figure S2**. **(D)** MeRIP-seq detected the m6A abundance of *Trub2* mRNA in the HFD group and HB group. The yellow highlight showed that the intensity of m6A peak was significantly higher in the HB group than in the HFD group. **(E)** The protein level of *Trub2* in the liver of CK, HFD, HB mice ($n = 3$). Gel images were cropped, and the original gels were presented in Supplementary **Figure S3**. **(F)** Quantitative results of *Trub2* protein levels. **(G-H)** Western blot analysis was employed to assess and quantify the expression efficiency of *Trub2* in OA/PA-treated AML12 cells after its overexpression ($n = 4$). Gel images were cropped, and the original gels were presented in Supplementary **Figure S4**. **(I)** Triglyceride levels in AML12 cells after transfected with *Trub2* after OA/PA treatment ($n = 3$). **(J)** Triglyceride content in AML12 cells after transfected with siNC and siTrub2 ($n = 6$). The data were expressed as the mean ± SD. $^{*}P < 0.05$, $^{**}P < 0.01$, $^{****}P < 0.0001$. CK, Control mice; HFD, High fat diet; HB, High fat diet with betaine.

Gene mRNA-level regulation by m6A modification

To identify key genes alleviating MASLD, we analyzed differentially methylated and expressed genes in HFD and HB groups. After filtering out genes with insignificant differences in m6A abundance and mRNA expression, 27 genes showed significant differences, suggesting they may be regulated by m6A modification. Among them, 11 transcripts showed m6A hypermethylation and up-regulated expression (Hyper-up), 13 transcripts displayed m6A hypermethylation and down-regulated expression (Hyper-down), no transcripts exhibited m6A hypomethylation and up-regulated expression (Hypo-up), and 3 transcripts had m6A hypomethylation and down-regulated expression (Hypo-down) (Fig. 4A). To assess the reliability of the RNA-seq data, five genes (*Appl1*, *Ntrk2*, *Cbx4*, *Trub2* and *Tlr4*) were randomly selected from 27 DEGs for validation by RT-PCR. Consistently, the mRNA levels of *Appl1*, *Ntrk2*, and *Trub2* were increased, while *Cbx4* and *Tlr4* mRNA levels were decreased in the HB group compared to the HFD group (Fig. 4B).

To understand the changes in m6A modification caused by betaine treatment, RNA m6A dot blot was performed to measure the levels of m6A modification. The results revealed that the m6A levels were increased in liver tissues of mice treated with betaine (Fig. 4C). Interestingly, some genes involved in mRNA processing showed significant elevations in m6A methylation and mRNA expression. For example, *Trub2*, which is associated with mRNA processing, had significantly higher m6A methylation and mRNA levels in the HB group than in the HFD group (Fig. 4D). Further examination showed that the protein level of *Trub2* was significantly increased in the HB group compared with that in the HFD group (Fig. 4E-F). We selected *Trub2*, a Hyper-up gene not previously reported to be involved in MASLD progression, as a candidate gene for further analysis.

Betaine reduces intracellular TG levels by regulating *Trub2* expression

To further verify the role of *Trub2* in betaine attenuating MASLD, *Trub2* was overexpressed in AML12 cells, and its expression level was detected by RT-PCR (Figure S1A). The protein levels of *Trub2* were significantly elevated in AML12 cells treated with OA/PA after overexpression of *Trub2* (Fig. 4G-H). Notably, intracellular TG was significantly reduced after *Trub2* overexpression in AML12 cells (Fig. 4I). This result reveals that *Trub2* is a novel target for regulating hepatic lipid metabolism. In addition, inhibition of *Trub2* increased intracellular TG levels in AML12 cells, and this increase was attenuated by betaine (Fig. 4J, Figure S1B). These results demonstrate that betaine inhibits intracellular TG accumulation by increasing *Trub2* expression.

In summary, betaine increases *Trub2* mRNA levels by enhancing its m6A methylation level and the stability of the mRNA, and this results in a reduction of intracellular TG level, thereby exerting a favorable influence on the improvement of MASLD (The whole article is summarized in Fig. 5).

Discussion

Betaine is a crucial natural methyl donor that plays a significant role in metabolism and liver function. Recent research has highlighted its active role in fat metabolism. The main objectives of this project are to explore betaine's potential in alleviating hepatic steatosis and to map m6A RNA methylation. This study provides insights into betaine's biological function in liver fat metabolism and its regulatory mechanisms, offering a solid scientific basis for its application in treating MASLD.

Our study supports the notion that differences in m6A modifications between HFD and HB groups significantly affect the expression of lipid metabolism-related genes. GO functional enrichment analysis showed that m6A-modified genes were enriched in processes like the MAPK cascade, Notch receptor target transcription, and dose compensation (Fig. 1C). Notably, pathways involving positive regulation of MAPK cascades and phosphatidylinositol phosphate phosphatase activity contained many differentially methylated genes, highlighting m6A methylation's role in regulating lipid metabolism and deposition. This enhances our understanding of fat metabolism and provides insights into the mechanisms of m6A methylation.

Moreover, KEGG pathway enrichment analysis revealed that downmethylated mRNAs were linked to several critical pathways, including the Wnt signaling pathway, animal autophagy, neurotrophic factor signaling, renal cell carcinoma, TGF-β pathway, mRNA surveillance, and cAMP signaling (Fig. 1E). The Wnt signaling pathway is mostly inactive in mature healthy livers, but it is consistently overactivated during cell renewal or regeneration, as well as in liver fibrosis, cirrhosis, and liver cancer[41]. In our study, the Wnt pathway in the betaine group showed downregulated mRNA m6A methylation, suggesting that betaine might mitigate fatty liver and prevent progression to liver cirrhosis and cancer by reducing m6A methylation of Wnt pathway-related mRNA-a novel

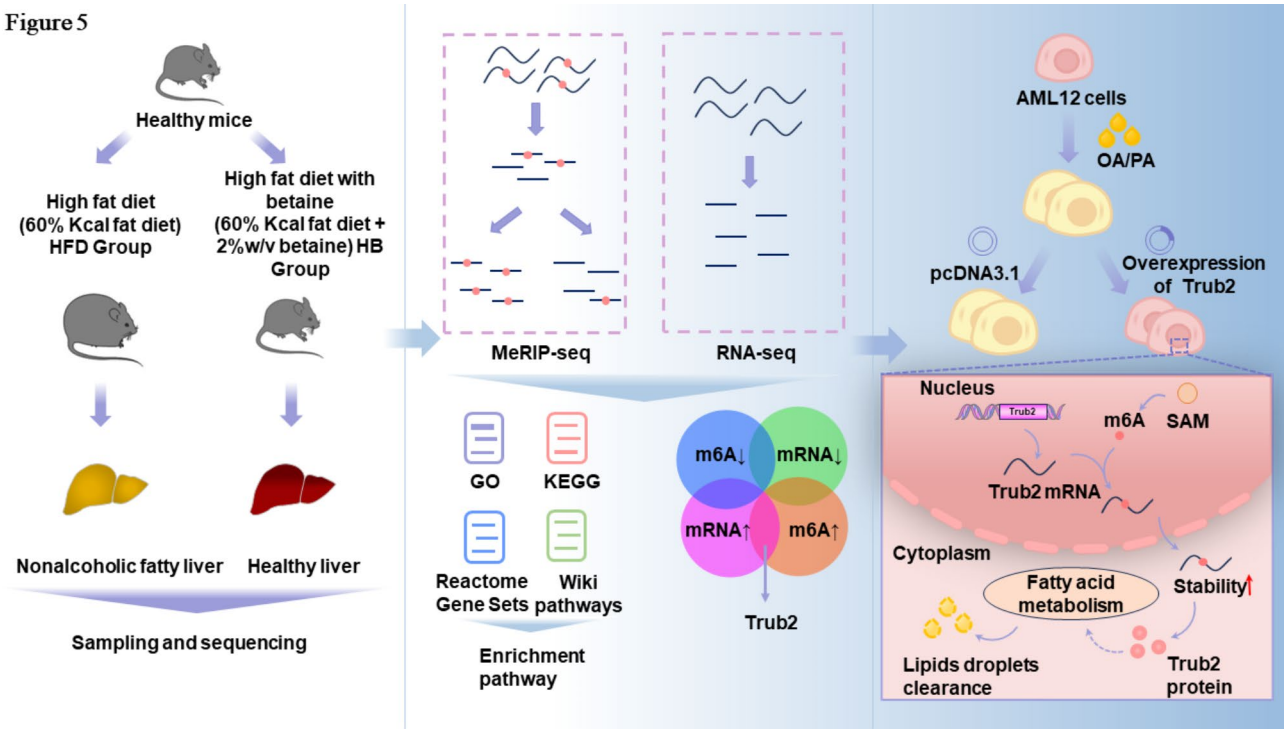

Fig. 5. Overview of the experimental design, analysis and validation. The graph showed that by combining RNA-seq and MeRIP-seq, we found many candidate genes related to lipid metabolism, including *Trub2*, and the major enrichment pathways such as mTOR signaling pathway, Rap1 signaling pathway and MAPK signaling pathway. These potential candidate genes and pathways are critical to understanding the beneficial effects of betaine production, and further research is needed to determine the precise processes by which they alleviate metabolic dysfunction-associated steatotic liver disease. In conclusion, this study provides a new resource for determining the remission effect of betaine on metabolic dysfunction-associated steatotic liver disease.

finding. While downmethylated mRNA holds significant research value for studying liver fat deposition, we surmise that these pathways do not play a dominant role in our context. Therefore, we investigated mRNA with upregulated methylation for further insights.

We found that upmethylated mRNAs are strongly associated with a variety of biological pathways, including biotin metabolism, lysine degradation, Rap1 signaling pathway, mTOR signaling pathway, and adhesion junction (Fig. 1B). The J Pearce's study illustrates the relationship between biotin deficiency and liver metabolism with fatty liver and renal syndrome[42]. Non-histone lysine crotonization is involved in the regulation of browning of white fat[43]. In DiZhang's study, thymoquone was successfully shown to improve glucose homeostasis through AMPK/mTOR/ULK1-dependent pathways, alleviate hepatic fatty acid salt disease, and reduce hepatic lipid accumulation associated with autophagy induction in mice fed a high-fat diet[44]. In comparison to the downmethylated mRNA pathway, we found that the upmethylated mRNA biological pathway in this experiment may exhibit a more prominent performance. By KEGG pathway enrichment analysis, we further explored the biological pathway affecting mRNA methylation level, thus providing a foundation for us to specifically explore how m6A affects liver fat deposition or metabolism.

In this study, the HFD and HB groups showed significant differences at the mRNA level. We concentrated on discerning the disparities in expression between the two cohorts, with the aim of elucidating the underlying biological mechanisms and implications (Fig. 2A). From a molecular standpoint, GO functional enrichment analysis highlighted that the upregulated mRNA was largely concentrated within processes involving lipid biosynthesis, small molecule biosynthesis, and both lipid and small molecule metabolism (Fig. 2B-E). This led to an acceleration of liver lipid metabolism and a reduction in TG levels in liver cells. Our study also shows that m6A methylation modification does play a very crucial role in lipid metabolism, and further proves that m6A may regulate gene expression through methylation modification, thereby affecting fat deposition metabolism.

In further research, we have uncovered those co-expressed genes enriched in several key pathways associated with negative regulation of phosphorus metabolism, alcoholic fatty liver disease, lipid metabolism genes, as well as vitamin and cofactor metabolism, show significant perturbations at both the m6A and mRNA levels in the betaine-treated group (Fig. 3A-F). We speculated that these pathways may indicate that under the influence of betaine, lipogenesis is significantly suppressed. Consequently, betaine holds potential therapeutic value in terms of promoting lipid metabolism and preventing the development of MASLD. This study provides robust theoretical backing for the application of betaine in the treatment of fatty liver conditions.

27 candidate genes affected by betaine therapy in MASLD models have been screened out. Interestingly, the Appl1-rs4640525 variant has been proved to be associated with MASLD, with the C allele being more prevalent in individuals with MASLD compared to the controls[45]. However, the mechanisms by which *Appl1* regulates MASLD have not been fully reported. It has been hypothesized that SNPs may influence *Appl1* expression levels, thereby altering adiponectin activity. Such alterations in adiponectin activity could subsequently lead to reduced fatty acid oxidation, potentially contributing to the development of fatty liver[46]. In addition, betaine treatment reduced serum TC and TG levels and the expression of *Tlr4*in HFD-induced MASLD rats[47]. These results suggest the beneficial efficacy of betaine and the reliability of the candidate genes.

Multiple studies have demonstrated the critical role of m6A modification in the regulation of mRNA stability, splicing, transport, localization, and translation. For instance, the m6A demethylase ALKBH5 facilitates m6A demethylation of glucose transporters type 4 (GLUT4) mRNA and enhances its stability in a YTHDF2-dependent manner[48]. Furthermore, m6A methylation is associated with mRNA degradation, which is mainly manifested as reduced stability of the transcript[49]. During the investigation of differential m6A peaks, we unexpectedly discovered that the *Trub2* gene transcript level was markedly overexpressed in the livers of betaine-treated mice, challenging our previous understanding of the *Trub2* gene and presenting a fresh avenue for exploring the related mechanisms of MASLD. Historically, the *Trub2* gene has been primarily associated with pseudouridine synthase activity, contributing to the positive regulation of mRNA pseudouridine synthesis and mitochondrial translation, and functioning either upstream or within mRNA and tRNA processing events. At the cellular level, overexpression of *Trub2* significantly decreased the triglyceride content of OA/PA treated cells (Fig. 4I). From a molecular biology standpoint, it seems plausible that the enhanced methylation level of m6A might promote the functional expression of *Trub2*, thereby boosting mitochondrial function and lipid metabolism. This finding reiterates the significance of m6A in modulating mRNA stability via methylation and underscores its pivotal role in regulating the expression of lipid-associated genes.

In summary, this project has further solidified the role of betaine in mitigating MASLD and elucidated the mechanism by which betaine alleviates MASLD through the lens of m6A methylation, successfully constructing an m6A methylation landscape. More notably, we have also identified a novel candidate gene, *Trub2*, which furnishes a fresh target for studying MASLD.

Remarkably, betaine, being a naturally occurring amino acid derivative ubiquitous in nature, exhibits distinctive biochemical properties and low cost, rendering it a potential therapeutic agent for treating MASLD. This suggests its potential to become a transformative intervention for MASLD patients and presents exciting prospects for future development. As applied sciences continue to evolve, we are justified in believing that betaine will assume an increasingly pivotal role in the management of MASLD, offering a ray of hope to the multitude of affected patients.

Data availability

The data that support the findings of this study are available from the corresponding author upon reasonable request. Some data may not be made available because of privacy or ethical restrictions. To review GEO accession GSE174550: Go to https://www.ncbi.nlm.nih.gov/geo/query/acc.cgi?acc=GSE174550.

Received: 19 August 2024; Accepted: 21 February 2025
Published online: 01 March 2025

References

1. YIN, X. et al. Glucose fluctuation increased hepatocyte apoptosis under lipotoxicity and the involvement of mitochondrial permeability transition opening [J]. *J. Mol. Endocrinol.* **55** (3), 169–181 (2015).
2. JAMES O F, DAY, C. P. Non-alcoholic steatohepatitis (NASH): a disease of emerging identity and importance [J]. *J. Hepatol.* **29** (3), 495–501 (1998).
3. XU, R. et al. *Recent Advances in Lean NAFLD [J]*153 (Biomedicine & Pharmacotherapy, 2022).
4. MOORE, E. & PATANWALA, I. A systematic review and meta-analysis of randomized controlled trials to evaluate plant-based omega-3 polyunsaturated fatty acids in nonalcoholic fatty liver disease patient biomarkers and parameters [J]. *Nutr. Rev.* **82** (2), 143–165 (2024).
5. ZHOU, F. et al. Unexpected rapid increase in the burden of NAFLD in China from 2008 to 2018: A systematic review and Meta-Analysis [J]. *Hepatology* **70** (4), 1119–1133 (2019).
6. DOMINISSINI D, MOSHITCH-MOSHKOVITZ S, SCHWARTZ, S. et al. Topology of the human and mouse m6A RNA methylomes revealed by m6A-seq [J]. *Nature* **485** (7397), 201–206 (2012).
7. ROUNDTREE I A, EVANS M E, PAN, T. et al. Dynamic RNA modifications in gene expression regulation [J]. *Cell* **169** (7), 1187–1200 (2017).
8. WU, J. et al. Emerging role of m6A RNA methylation in nutritional physiology and metabolism [J]. *Obes. Rev.*, **21**(1). (2019).
9. RIES R J, Z. A. C. C. A. R. A. S. & JAFFREY, S. R. Reading, writing and erasing mRNA methylation [J]. *Nat. Rev. Mol. Cell Biol.* **20** (10), 608–624 (2019).
10. HYUN, K. et al. Writing, erasing and reading histone lysine methylations [J]. *Exp. Mol. Med.* **49** (4), e324–e (2017).
11. CHEN, J. et al. FTO-dependent function of N6-methyladenosine is involved in the hepatoprotective effects of betaine on adolescent mice [J]. *J. Physiol. Biochem.* **71** (3), 405–413 (2015).
12. HU, Y. et al. Demethylase ALKBH5 suppresses invasion of gastric cancer via PKMYT1 m6A modification [J]. *Mol. Cancer*, **21**(1). (2022).
14. MU, H. et al. RNA binding protein IGF2BP1 meditates oxidative stress-induced granulosa cell dysfunction by regulating MDM2 mRNA stability in an m6A-dependent manner [J]. [*Redox Biol.*, 57. (2022)102492/102492]." Redox biology vol. 67 (2023): 102880.
14. CRAIG S A S. *Betaine in Human Nutrition [J]*80539–549 (AMERICAN JOURNAL OF CLINICAL NUTRITION, 2004). 3.
15. ZHAO, G. et al. *Betaine in Inflammation: Mechanistic Aspects and Applications [J]*9 (Frontiers in Immunology, 2018).
17. DAY C R, KEMPSON, S. A. Betaine chemistry, roles, and potential use in liver disease [J]. Biochimica et biophysica acta vol. 1860,6 (2016): 1098-106.
17. ARUMUGAM M K et al. *Beneficial Eff. Betaine: Compr. Rev. [J] Biology*, **10**(6). (2021).

19. ABDELMALEK M F, SANDERSON S O, A. N. G. U. L. O. P. et al. vol 50, pg 1818,. Betaine for Nonalcoholic Fatty Liver Disease: Results of a Randomized Placebo-Controlled Trial [J]. HEPATOLOGY, 2010, 51(5): 1868-. (2009).
19. HUANG, T. et al. Integrated transcriptomic and Translatomic inquiry of the role of betaine on lipid metabolic dysregulation induced by a High-Fat diet [J]. *Front. Nutr.*, 8. (2021).
20. VALENTIM A M et al. Euthanasia using gaseous agents in laboratory rodents [J]. *Lab. Anim.* **50** (4), 241–253 (2016).
21. WAGNER, G. P. & LYNCH, K. I. N. K. Measurement of mRNA abundance using RNA-seq data: RPKM measure is inconsistent among samples [J]. *Theory Biosci.* **131** (4), 281–285 (2012).
22. KANEHISA, M. et al. KEGG as a reference resource for gene and protein annotation [J]. *Nucleic Acids Res.* **44** (D1), D457–D462 (2016).
23. KANEHISA, M. KEGG: Kyoto encyclopedia of genes and genomes [J]. *Nucleic Acids Res.* **28** (1), 27–30 (2000).
24. MONTEIRO G A & DUARTE S O D The effect of Recombinant protein production in Lactococcus lactis transcriptome and proteome [J]. *Microorganisms*, **10**(2). (2022).
25. MITAKA, T. et al. Growth and maturation of small hepatocytes [J]. J Gastroenterol Hepatol, 13 Suppl: S70-7. (1998).
26. RAMANATHAN, R. & DELVAUX N A, RICE K, G. Gene transfection of primary mouse hepatocytes in 384-well plates [J]. *Anal. Biochem.* **644**, 113911 (2022).
27. ĆOROVIĆ, A. et al. Somatostatin receptor PET/MR imaging of inflammation in patients with large vessel vasculitis and atherosclerosis [J]. *J. Am. Coll. Cardiol.* **81** (4), 336–354 (2023).
28. MEYER KATE D, SALETORE, Y. et al. Comprehensive analysis of mRNA methylation reveals enrichment in 3′ UTRs and near stop codons [J]. *Cell* **149** (7), 1635–1646 (2012).
29. PAUL, B., LEWINSKA, M. & ANDERSEN, J. B. Lipid alterations in chronic liver disease and liver cancer [J]. *JHEP Rep.*, **4**(6). (2022).
30. BEDI, O. et al. Molecular and pathological events involved in the pathogenesis of Diabetes-Associated nonalcoholic fatty liver disease [J]. *J. Clin. Experimental Hepatol.* **9** (5), 607–618 (2019).
31. ZHANG S F, Y. A. N. L. S. et al. Schisandrin B mitigates hepatic steatosis and promotes fatty acid oxidation by inducing autophagy through AMPK/mTOR signaling pathway [J]. *Metabolism-Clinical Experimental*, 131. (2022).
32. LI, J. et al. CD147 reprograms fatty acid metabolism in hepatocellular carcinoma cells through Akt/mTOR/SREBP1c and P38/PPARα pathways [J]. *J. Hepatol.* **63** (6), 1378–1389 (2015).
33. LIU, H. et al. Deletion of Telomere-Rap1 aggravated cardiac aging by imparing fatty acid oxidation < i > via PPARα signaling [J]. *FASEB J.*, 33. (2019).
34. QIN G H, MA, J. et al. *Isoquercetin Improves Hepatic Lipid Accumulation by Activating AMPK Pathway and Suppressing TGF-β Signaling on an HFD-Induced Nonalcoholic Fatty Liver Disease Rat Model [J]*19 (INTERNATIONAL JOURNAL OF MOLECULAR SCIENCES, 2018). 12.
35. YANG, W. et al. Regulation of cholesterol metabolism during high fatty acid–induced lipid deposition in calf hepatocytes [J]. *J. Dairy Sci.* **106** (8), 5835–5852 (2023).
36. HWANG, J. L. & WEISS R E. Steroid-induced diabetes: a clinical and molecular approach to Understanding and treatment [J]. *Diab./Metab. Res. Rev.* **30** (2), 96–102 (2014).
37. SABARI B R, ZHANG, D. et al. Metabolic regulation of gene expression through histone acylations [J]. *Nat. Rev. Mol. Cell Biol.* **18** (2), 90–101 (2016).
38. HOLLAND A M et al. Testosterone inhibits expression of lipogenic genes in visceral fat by an estrogen-dependent mechanism [J]. *J. Appl. Physiol.* **121** (3), 792–805 (2016).
39. XIE, F. et al. Estrogen mediates an Atherosclerotic-Protective action via Estrogen receptor Alpha/SREBP-1 signaling [J]. *Front. Cardiovasc. Med.*, 9. (2022).
40. MENDOZA, A. et al. Controlled lipid β-oxidation and carnitine biosynthesis by a vitamin D metabolite [J]. *Cell. Chem. Biology*. **29** (4), 660–9e12 (2022).
41. MONGA, S. P. β-Catenin signaling and roles in liver homeostasis, injury, and tumorigenesis [J]. *Gastroenterology* **148** (7), 1294–1310 (2015).
42. PEARCE, J. Biotin deficiency and liver metabolism in relation to fatty liver and kidney syndrome [J]. *Br. Poult. Sci.* **19** (4), 431–439 (1978).
43. LIU, Y. et al. Non-Histone lysine crotonylation is involved in the regulation of white fat Browning [J]. *Int. J. Mol. Sci.*, **23**(21). (2022).
44. ZHANG, D. et al. Thymoquinone attenuates hepatic lipid accumulation by inducing autophagy via AMPK/mTOR/ULK1-dependent pathway in nonalcoholic fatty liver disease [J]. *Phytother. Res.* **37** (3), 781–797 (2022).
45. WANG, B. et al. Association of APPL1 gene polymorphism with Non-Alcoholic fatty liver disease susceptibility in a Chinese Han population [J]. *Clin. Lab.* **61** (11), 1659–1666 (2015).
46. BARBIERI, M. et al. Association of genetic variation in adaptor protein APPL1/APPL2 loci with non-alcoholic fatty liver disease [J]. *PloS One*. **8** (8), e71391 (2013).
47. ZHANG, W. et al. Betaine protects against High-Fat-Diet-Induced liver injury by Inhibition of High-Mobility group box 1 and Toll-Like receptor 4 expression in rats [J]. *Dig. Dis. Sci.* **58** (11), 3198–3206 (2013).
48. LIU, H. et al. ALKBH5-Mediated m6A demethylation of GLUT4 mRNA promotes Glycolysis and resistance to HER2-Targeted therapy in breast Cancer [J]. *Cancer Res.* **82** (21), 3974–3986 (2022).
49. ZHOU, B. et al. N6-Methyladenosine reader protein YT521-B homology Domain-Containing 2 suppresses liver steatosis by regulation of mRNA stability of lipogenic genes [J]. *Hepatology* **73** (1), 91–103 (2020).

Acknowledgements

This work was supported by National Natural Science Foundation of China (32272952 and 82460174); Guangxi Science Foundation for Distinguished Young Scholars (2020GXNSFFA297008); Guangxi Academy of Medical Sciences high-level Talents Foundation (YKY-GCRC-202302);and National College Students Innovation and Entrepreneurship Training Program (202110593147 and 202310593446).

Author contributions

Conceptualization, L.Z. and Y. L. ; Data curation, L.Z. and Y. L. ; Formal analysis, Y.W., J.Y., H.S. and D.L. ; Funding acquisition, Y.W. and L.Z. ; Investigation, Y.W., J.Y., H.S., D.L., Z.L., X.L. and Z.D. ; Methodology, J.Y., L.Z. and Y.L. ; Project administration, Y.L. ; Resources, Y.Z. and Y.L. ; Supervision, Y.L. ; Validation, Y.W., J. Y., H.S., D.L., Z.L., X.L. and Z.D. ; Visualization, Y.W., J.Y., H.S., D.L. and Z.L. ; Writing – original draft, Y.W. ; Writing – review & editing, Y.L. .

Declarations

Competing interests
The authors declare no competing interests.

Additional information
Supplementary Information The online version contains supplementary material available at https://doi.org/10.1038/s41598-025-91573-0.

Correspondence and requests for materials should be addressed to Y.L.

Reprints and permissions information is available at www.nature.com/reprints.

Publisher's note Springer Nature remains neutral with regard to jurisdictional claims in published maps and institutional affiliations.